



A phenomenological study of the timing of solar activity minima of the last millennium through a physical modeling of the Sun–Planets Interaction



Rodolfo Gustavo Cionco^{a,*,1}, Willie Soon^b

^aGrupo de Estudios Ambientales, Universidad Tecnológica Nacional, Colón 332, San Nicolás (2900), Bs.As., Argentina

^bHarvard-Smithsonian Center for Astrophysics, Cambridge, MA 02138, USA

HIGHLIGHTS

- A physical model of Sun–Planets Interaction is described.
- Solar activity Grand Minima (GM) are related to the Sun's closest approaches to barycenter.
- There are several candidate GM events in the next 1000 yr.

ARTICLE INFO

Article history:

Received 18 April 2014

Received in revised form 13 June 2014

Accepted 2 July 2014

Available online 10 July 2014

Communicated by Jun Lin

Keywords:

Sun–Planets Interaction

Solar inertial motion

Solar activity Grand Minima

ABSTRACT

We numerically integrate the Sun's orbital movement around the barycenter of the solar system under the persistent perturbation of the planets from the epoch J2000.0, backward for about one millennium, and forward for another millennium to 3000 AD. Under the Sun–Planets Interaction (SPI) framework and interpretation of Wolff and Patrone (2010), we calculated the corresponding variations of the most important storage of the specific potential energy (PE) within the Sun that could be released by the exchanges between two rotating, fluid-mass elements that conserve its angular momentum. This energy comes about as a result of the roto-translational dynamics of the cell around the solar system barycenter. We find that the maximum variations of this PE storage correspond remarkably well with the occurrences of well-documented Grand Minima (GM) solar events throughout the available proxy solar magnetic activity records for the past 1000 yr. It is also clear that the maximum changes in PE precede the GM events in that we can identify precursor warnings to the imminent weakening of solar activity for an extended period. The dynamical explanation of these PE minima is connected to the minima of the Sun's position relative to the barycenter as well as the significant amount of time the Sun's inertial motion revolving near and close to the barycenter. We presented our calculation of PE forward by another 1000 yr until 3000 AD. If the assumption of the solar activity minima corresponding to PE minima is correct, then we can identify quite a few significant future solar activity GM events with a clustering of PE minima pulses starting at around 2150 AD, 2310 AD, 2500 AD, 2700 AD and 2850 AD.

© 2014 Elsevier B.V. All rights reserved.

1. Introduction

The study of solar magnetic variability through the magnetohydrodynamic dynamo mechanisms of α – Ω or the helicity-differential rotation effects on the rotating and convecting fluid motions within the Sun has been a fruitful direction in pointing out the various non-linear aspects of the solar activity behavior, including extended

time intervals of activity minima (see Gough, 1990; Tobias et al., 1995; Gough, 2002; Usoskin et al., 2007; Spiegel, 2009; Jouve et al., 2010; Weiss, 2011; Choudhuri and Karak, 2012; Pipin et al., 2012; Brandenburg, 2013; Olemskoy and Kichatinov, 2013; Usoskin, 2013; Augustson et al., 2014; Passos et al., 2014). Pipin et al. (2012) found recently that a combination of the random fluctuations of the dynamo governing parameters and the nonlinear relaxation of the principal dynamo mechanisms can produce quasi-periodic variations on multidecadal to millennial timescales. In general, the solar dynamo theory supports the idea that long-term quasi-periodic variations of solar magnetic activity can result

* Corresponding author.

E-mail addresses: gcionco@frsn.utn.edu.ar (R.G. Cionco), wsoon@cfa.harvard.edu (W. Soon).

¹ Principal corresponding author.

from the nonlinear interplay between the magnetic field, differential rotation and helical convective motions. The most important timescales are related to the time taken to re-establish the angular momentum balance (differential rotation) and the hydrodynamic and magnetic helicity balance (associated with the α -effect) in the convection zone caused by perturbations in the large-scale magnetic field. Both processes, i.e. relaxation of the angular momentum transport and the magnetic helicity balance, operate on timescale roughly of about 10 sunspot cycles (see, Pipin, 1999; Pipin et al., 2012). However, the stability of the revealed periods can be questioned, because the dynamo may become non-stationary under the random fluctuations. Moreover, it happens that the dynamical properties of the solar dynamo on the millennial timescale look very similar to the properties of the Brownian motions (Pipin et al., 2013). In the words of Stenflo (2013): “This shows that the simplistic phenomenological model of coherence flux ropes needs to be replaced by a dynamo scenario in which fluctuations on all scales play a major role”. This is why the current explanations for the solar activity variations are far from adequate especially considering the fact that most of the parametric dynamo modeling efforts lack the exact specificity in the actual time domain and time arrow for the occurrences of various solar activity minima or Grand Minima, GM, that included the so-called Oort, Wolf, Spörer, Maunder and Dalton minima (hereafter abbreviated as OM, WM, SM, MM and DM) covering known records for the past 1000 yr or so.

In this paper, we propose to study and explore solar activity’s “prolonged” minima (in the sense described rather well by E. W. Maunder as early as 1894 (Maunder, 1894); see further discussion in Soon and Yaskell, 2004) occurred during the past ~ 1000 yr and Sun–Planets Interaction, SPI. To be sure, several past works (see Jose, 1965; Fairbridge and Shirley, 1987; Gokhale, 1998; Landscheidt, 1999; Charvátová, 2000; Juckett, 2000; Javaraiah, 2005; Paluš et al., 2007; Charvátová, 2009; Wolff and Patrone, 2010; Perryman and Schulze-Hartung, 2011; Scafetta, 2012; Tan and Cheng, 2013) have made some important attempts and progress although some of these works focused on different issues and questions than our current work. We based our theoretical study focusing on the well known GM events of the last millennium by adopting the most recently available reconstruction of the proxy sunspot number, by Usoskin et al. (2014). These authors emphasized that a better knowledge and quantitative information on the past geomagnetic activity (Licht et al., 2013) are necessary if we are to extend the secure knowledge of past solar activity variation back 10,000 yr in the past.

We begin our study by performing accurate numerical integration of the Sun’s motion around the barycenter of the solar system under the perturbations of the orbiting planets for 1000 yr, into the past. Next, we assume a physical connection between the Sun and planets by adopting the new framework outlined by Wolff and Patrone (2010, WP10). Although the WP10 mechanism involves specific assumptions, we speculate that the most complete SPI mechanisms that modulate the internal properties and limits the operation of the solar dynamo may arise through the modulation of the hydrodynamic helicity parameter. We postulate that the persistent pulses of the storage PE variations may lead to a significant perturbation of the turbulent helicity, i.e., significant quenching of the α -effect that is the standard ingredient for solar dynamo in explaining nonlinear modulation of the solar magnetic variability. Interestingly, Hazra et al. (2014) and Passos et al. (2014) recently commented that both the surface- and deeper solar interior-based sources of α -effect are important and necessary for their models of solar dynamo activity to enter and exit a Maunder-like GM event. In this sense, our proposed mechanism is not to replace the well-founded physical processes of the solar dynamo but instead our new interpretation is that the adopted SPI mechanism may be phenomenologically useful in explaining the well-observed

occurrences of these well-documented, past solar activity GM events. What the SPI assumption offers is that the host of quasi-regular oscillations of the observed solar activity variations of the last millennium can be naturally explained given the realistic and persistent nature of the external perturbations imposed on the Sun’s internal dynamics by the orbiting planets.

The WP10 theory relies on interchange arguments; i.e., a fluid element (a “cell”) is composed of two sub-masses (separated by a radius of gyration R_g) which by interchanging their positions, can store and release PE but conserving angular momentum. This PE storage mechanism is created owing to the rotating star, even if it is solidly rotating, combined with its barycentric motion. The possibility of release this energy is related to pre-existing internal flows of fluid motions. Although the applicability of WP10 mechanism in a real star clearly need specific requirements to be met (e.g., Cionco, 2012), this is the first mechanism devoted to explain modifications of stellar interiors by planetary gravitational perturbations (i.e., taking only into account inertial movements). In this context, WP10 have shown that, of all the possibilities, the large storage of PE (and with the yet-to-be fully specified mechanisms for the release of this PE), can occur when the cell is favorably positioned in alignment to the Sun’s center and solar system barycenter direction, and more specifically for the mass elements to be located: (1) in the radiative mixed-shell zone ($0.16R_s$), (2) in the convective envelope ($\sim 0.8R_s$), and (3) in the tachocline ($0.68R_s$), with R_s being the Sun’s radius.

In a previous study, Cionco and Compagnucci (2012), focused on the effects within the mixed shell of the Sun’s radiative zone, and analyzed PE variations as a function of time but only from ~ 1600 AD to present. They do not take into account the full roto-translational dynamical evolution of a cell in this zone; they only considered the maximal variation of the PE stored in this fixed zone, while optimally directed toward the barycenter, as a function of the barycentric distance. This earlier work found important PE variations that just preceded the GM (i.e., Maunder and Dalton minima as determined by the inferred number of sunspots) of the 17th and 19th century, and also the current period of significantly weakened solar activity that centered at around Solar Cycle 24 (see e.g., Tan, 2011). These significant drops in sunspot activity were related with apparent solar system dynamical particularities (i.e., giant planets’ alignments) which produce a strong radial acceleration and prevented the Sun to properly loop around the barycenter in its normal prograde motion (i.e., when the solar motion is retrograde around the barycenter, see Charvátová, 2000, 2009).

However, as noted above, the available records of solar activity can be extended further back in time using the available Earth-based solar activity proxies like the measurements of cosmogenic isotopes ^{14}C in tree rings, ^{10}Be in ice cores, and even nitrate concentration in ice cores (see Soon et al., 2014). Furthermore, a full dynamical description of the solar system motions (i.e., translation around the barycenter and intrinsic rotation within the Sun) that takes into account of all three critical center of actions within the Sun where PE could be stored and released (i.e., $\text{PE} > 0$) has not yet been done. In this study, we added these two new crucial components for a more comprehensive examination of the relationships between PE variations and the timing of solar activity minima. We wish to explain that we only extend the available proxy solar activity record back to about 1000 yr (i.e., to about 900 AD) in the past because as highlighted above that more accurate information from past geomagnetic variations are necessary. Usoskin et al. (2014) suggested that for the proxy solar activity reconstructed from the ^{14}C record to agree with the independent reconstruction based on ^{10}Be record, one must not extend back to about 2000–3000 yr in the past. This is why we focus narrowly and conservatively on solar activity variations for the past millennium or so.

We propose that our SPI study fits well within the latest interests in the broad subject and general new framework of Star–Planets Interaction. Petigura et al. (2013) recently quantified, based on statistics accumulated from the *Kepler*'s mission, that $11 \pm 4\%$ of the Sun-like stars may harbor an Earth-sized planet receiving between one and four times the stellar irradiation intensity as that on Earth. Spiegel et al. (2010) speculated that the long-term climate habitability of planets around a Sun-like star may be ultimately depended on the detailed architecture of the planetary system hosted the central star. They showed that how a non-zero eccentricity of Jupiter orbit is a significant driver of Earth's orbital eccentricity and that if Jupiter's eccentricity in the distant past were much larger than now (0.04), Jupiter could force a much larger amplitude variation in Earth's eccentricity in that it would push a globally frozen, "snowball" Earth into a more habitable and warmer climatic state. Finally, Gizon et al. (2013) pointed out an important constraint on the asteroseismic signatures from the Sun-like star, HD 52266, being imposed by the presence of an exoplanet of about $1.85 M_J$ (M_J = Jupiter mass) situated about 0.5 a.u. from the central star. Finally, the SPI mechanism of WP10, in the case where the scenario for the optimal perturbation at the mixed shell centered around $0.16R_s$ borne out, predicted that the Sun may shine more brightly and hence has a shorter lifetime than the case of a central star without orbiting planets.

In Section 2, we present our modeling of the solar barycentric motion. We discuss our methods and assumptions of SPI interaction in details in Section 3. We discuss the result of our calculation of PE and our interpretation in Section 4. Finally, we conclude in Section 5.

2. The solar barycentric motion (SBM)

We have obtained solar barycentric position (\mathbf{r}_B), velocity ($\dot{\mathbf{r}}_B$) and acceleration by integrating the equation of motions of the Solar System planets from the fiducial J2000.0 epoch to about 900 AD, backward. This procedure, among other things, enable us to calculate and deduce a wide range of solar system dynamical variables at different times for several lapses of times at adequate (or even arbitrary) sampling times, with high accuracy. Indeed, the planetary equations of motions were integrated using *Mercury6.2* (Chambers, 1999) in high precision Bulirsch–Stoer mode. We used one Earth's day as initial time step, then the program chooses its optimal time step to meet the adopted tolerance (maximum error by timestep) of 1×10^{-15} . Initial conditions (ecliptical rectangular coordinates) were taken from JPL Horizons system at J2000.0 epoch (i.e., ecliptic and mean equinox of January 1st 2000, at noon of the Terrestrial Time in ICRF reference system).

We have also taken into account the new astronomical unit, a.u., definition and the newly determined solar mass as in JPL Horizons (1.988544×10^{30} kg). We considered only Newtonian interaction between the bodies (i.e., we neglected general relativity), and placed the Earth and the Moon mass in the barycenter of this "two-planets" system; this assumption is sufficient for our purposes because of the short time scale undertaken and because the Sun's barycentric movement is strongly coupled to movements of the giant planets. For completeness, our model includes the "figure acceleration" owing to the oblateness of the Sun characterized by the J_2 dynamical form-factor (the most important limiting factor on long-term ephemerid calculations), so the planets do experienced this acceleration and, as a consequence, the Sun felt an inertial reaction because of this acceleration. Therefore, our model is more than purely inertial, it take into account an approximation to the permanent dis-figure of the Sun. We adopted $J_2 = 1.8 \times 10^{-7}$ following the most recent specification by Fienga et al. (2013). With this procedure, the error in the Sun's barycentric position, compared with the newest JPL's DE431 ephemerides is better than 100 km in the

location of the Sun's center in 1000 yr. We also obtain the orbital elements that define the osculating solar barycentric orbit, and the Sun's acceleration decomposed in particular directions respect to solar orbit, which permits a clearer view of the planetary accelerations on Sun's movement (Cionco and Compagnucci, 2012).

3. Potential energy variations

One of the fundamental assumptions of WP10 is the co-planarity between Sun's equator and planetary movements. Although the solar barycentric movements described in the ecliptic system is basically planar (vertical z-movements are much smaller), but for a better fit to this assumption, we transform the solar coordinates obtained in Section 2 to the invariable plane of the solar system (Souami and Souchay, 2012).

For exploring the three possible zones of PE storage, WP10 used mainly cylindrical barycentric coordinates and they have taken only into account Sun's locations where the buoyancy force over the fluid cell can be neglected. Basically in the WP10 formalism there are two possible cases: when the plane of the overturning (plane where the mass interchange could take place) is in the direction of barycenter and when is not (see Fig. 1 in WP10). The first case coincides with the direction towards the barycenter (as observed from the cell), they labeled this case as "vertical"; in the second case, the interchange is performed at 90° from the local vertical line of the cell (line passing trough the Sun's center, the cell center and the barycenter), they labeled this case "horizontal". An angle (ϵ) measures the orientation between the overturning plane and the direction to the barycenter. In the vertical case, ϵ is always zero. In the horizontal case, $\epsilon \in (0, 90^\circ]$. These two cases take into account all the possible overturning planes or perturbations.

WP10 constructed parametric-space plots showing that, of the two cases, the largest positive values of PE (i.e., the maximum storage of available PE) are found in the vertical case. In this way, the PE stored is allocated in a zone facing the barycenter and the strongest storage is when the cell's barycentric position is near $0.75r_B$, where r_B is the barycentric distance of the Sun's center (see Fig. 1 here and Fig. 3 in WP10). Therefore, they suggested that this vantage location is more prone to instability. This position and all locations determined as fixed distances to the barycenter are continuously moving with respect to the Sun, i.e., they do not correspond to a well determined or a fixed solar zone.

For a more complete modeling of the dynamical evolution of PE values at different solar zones, we need to work in an heliocentric system to set a solar location and then follow the evolution of a cell in this location as it passes through different PE zones. For consistency with WP10 (see Fig. 1 in that paper), we adopted an heliocentric system oriented to the barycenter, then the position of a cell, in cylindrical coordinates, is $\mathbf{r}_H = (r_H, \theta)$ with θ angle measured from that direction to the barycenter (Fig. 1). Thus, θ is the angular position of a cell's center of gravity with reference to the barycenter direction. In our model, the Sun is treated as a body in rigid rotation; the cells are composed of two sub-masses which in turn have the possibility to interchange their positions and release the stored PE in the sense of WP10. Therefore, the temporal evolution of θ responds to both the barycentric (translational) and the stellar (rotational) dynamics, so this geometry can be easily described with the aid of another heliocentric system but oriented with respect to the inertial J2000.0 system (see Fig. 1):

$$\theta = \lambda_0 + \omega(t - t_0) \pm 180^\circ - \nu(t) \quad (1)$$

where λ_0 is the initial angular position (i.e., initial longitude) of a cell at the arbitrary time t_0 respect to the X_γ direction (pointing to γ vernal point of J2000.0); ω is the Sun's spin/rotation rate; $\nu(t)$ is the Sun's angular barycentric coordinate from the inertial X_γ line

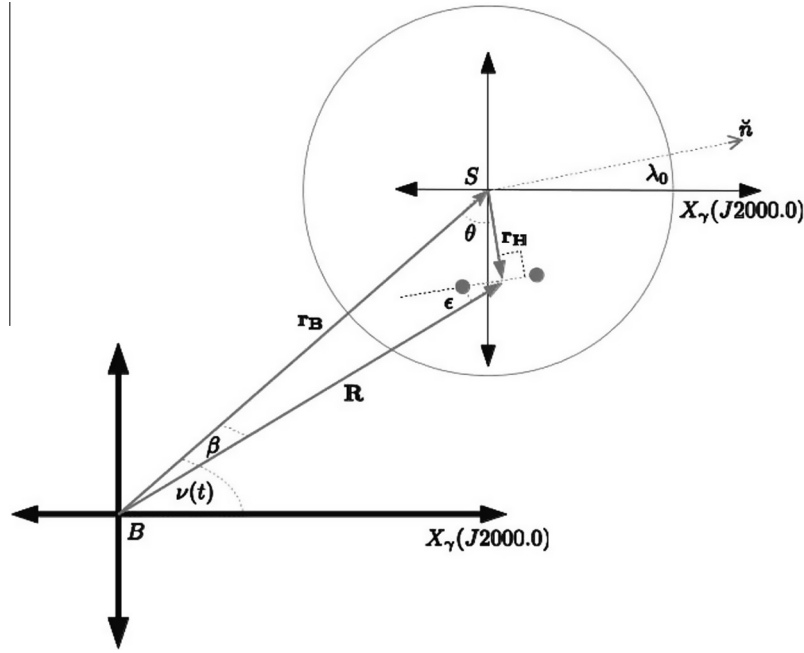


Fig. 1. A sketch of the reference systems used to evaluate the geometrical and dynamical quantities for the Sun–Planets Interaction (see text for a fuller description). *S* is the Sun center; *B* is the barycenter of the Solar System; λ_0 is the initial longitude of the cell with local vertical \hat{n} . The cell is depicted to consist of the two small spheres whose overturning plane has been drawn perpendicular to \mathbf{r}_H .

at time t . Now, following Eq. (12) of WP10, we can write the scalar field of PE in the vertical case (PE_v) as:

$$PE_v(r_h, \theta, t) = -8(\omega R_g)^2 (X^2 - 3X + 2) \quad (2)$$

where R_g is the radius of gyration mentioned above, and:

$$X = \mu \left[1 + \left(\frac{r_H}{r_B} \right)^2 - 2 \left(\frac{r_H}{r_B} \right) \cos \theta \right]^{-1/2} \quad (3)$$

$$\mu = \left(1 - \frac{\Omega}{\omega} \right) \cos \beta - \left(\frac{\dot{r}_B}{r_B \omega} \right) \sin \beta, \quad (4)$$

$\Omega = dv/dt$ is the instantaneous solar angular motion measured with reference to X_γ direction; and β is the angular position of the cell with respect to the Sun's center as seen from the solar system barycenter. The sense of θ direction is defined by $\sin \theta = +((-\mathbf{r}_B) \times \mathbf{r}_H)/r_B r_H$.

In the derivation of Eq. (2), we assume the barycentric dynamical quantities as function of time, then in order to make further calculations we need to: 1) fix the solar zone under study (set r_h), 2) set the initial longitude of the cell at the beginning of the calculation, 3) fix the time of the calculation (i.e., we obtain the barycentric motion of the Sun and the rotational state of the Sun as a function of θ).

For the horizontal case, the reader is referred to Eq. (17) in WP10, the calculations are more cumbersome and are not described in details here. The PE has a more complex dependence on R_g and also, it has to include the dependence on the inclination of the overturning plane with respect to the barycenter (ϵ), which is $\epsilon = 90 - \theta - \beta$. We call this field of PE as PE_h in our paper.

As mentioned in Section 1, the PE estimates were made by assuming a negligible buoyancy forcing at the three specific solar locations. Therefore, for an estimate of the total PE stored, PE_{tot} , we sum the PE available in the radiative zone, the tachocline and in the convective envelope where PE_{tot} stored as the solar system bodies evolve over time, t , is:

$$PE_{tot}(t) = PE_v(0.16R_s, t) + PE_v(0.8R_s, t) + PE_h(0.68R_s, t) \quad (5)$$

where each evaluation of the individual PE is obtained from the integration over the angle θ :

$$PE_v(0.16R_s, t) = \int_{\theta_1}^{\theta_2} PE_v(0.16R_s, \theta, t) d\theta \quad (6)$$

$$PE_v(0.8R_s, t) = \int_{\theta_3}^{\theta_4} PE_v(0.8R_s, \theta, t) d\theta \quad (7)$$

$$PE_h(0.68R_s, t) = \int_{\theta_5}^{\theta_6} PE_h(0.68R_s, \theta, t) d\theta \quad (8)$$

For the vertical case (Eqs. (6) and (7)), the integrands need to be evaluated from Eq. (2) by simply replacing r_h with $0.16R_s$ and $0.8R_s$ respectively. For the horizontal case (Eq. (8)), the integrand needs to be evaluated according to Eq. (17) in WP10, as already mentioned; in this expression, we have also replaced the radial variable r_h with $0.68R_s$ corresponding to the tachocline location.

Finally, the integral limits are set by taking into account the zones where $PE > 0$ (i.e., where the energy is available for release) at each given time.

4. Results and discussion

WP10 have only shown the instantaneous values of PE, from the assumed and averaged solar dynamics parameters. Therefore, it is important to take into consideration all possible values from the solar barycentric motion, in particular the effect of ever-changing and varying Ω/ω ratio.

We solve the integrals (6)–(8) numerically by quadrature, using an iterative scheme. Beginning with a step $\Delta\theta^1$ we calculate a value PE^1 , then we refine the θ -partition and obtain a value PE^2 and stop the algorithm if $|PE^2 - PE^1| < 10^{-5}$. Fig. 2 shows PE_{tot} values as a function of time, i.e., the contribution of all PE available summed at the three key zones proposed in WP10, covering several of the historically known periods with solar activity Grand Minima, GM, events. PE values are expressed in non-dimensional

(arbitrarily-scaled) units, so only the relative change in the values of PE is meaningful for physical interpretations.

These PE values oscillate depending mainly on the r_B distances. The basic period presents in PE series are the orbital period of Jupiter, the Jupiter–Saturn synodic period (J–S) and the Saturn–Uranus synodic period (S–U). Their averaged values as obtained directly from our simulations are: 11.87 yr, 19.84 yr, 45.45 yr, respectively. They are not “exactly present” in time domain because these giant planets are perturbing each other; e.g. Jupiter modifies S–U period subtly as will be further explained below. PE_{tot} follows essentially the behavior of $PE_v(0.16R_s, t)$ because the contributions from the two other zones are relatively smaller. The tachocline contribution is about 10^{-3} of the “averaged normal values” of $PE_v(0.16R_s, t)$ and the contribution from convective envelope zone has only sporadic peaks of $PE > 0$ that never surpass the maximum values of $PE_v(0.16R_s, t)$. The solar barycentric motion never produces barycentric distances large enough to move the maximum values of PE available into the convective envelope zone (see Fig. 3 in WP10). Indeed, most of the time the convective envelope (and outer layer of the Sun) has no storage of PE.

Nevertheless, every ~ 179 yr the giant planets quasi-alignments (Javaraiah, 2005) produce the closest approaches to the barycenter, as shown by the important PE_{tot} drops in Fig. 2. These are times when the minimum of PE is stored in the Sun. Basically, what happens is that PE_v maxima dip into deeper zones (deeper than $0.16R_s$), when r_B is lesser than $\sim 0.65R_s$, whereas the PE in the tachocline is never depleted and always preserve an amount of PE as was previously explained (i.e. PE_{tot} is never zero).

Our calculated ratios for the translational–rotational parameter, Ω/ω , are depicted in Fig. 2. Our independent calculations confirm the mean value of 0.0045 adopted by WP10 in their works. We also find the maximum values that surpassed 0.07 (in absolute value) at certain epochs; these high values, however, has only a small net effect of reducing the total PE values by a very small quantity. The well known times of solar retrograde motion, i.e., around ~ 1632 AD, 1811 AD, 1990 AD, yielded negative values of Ω/ω . It is important to note that all the spikes in Ω/ω are produced only by (more-or-less pronounced) minima in r_B , whereas big drops in

PE_{tot} are produced only by the closest approaches to the barycenter. The Ω/ω ratio, which expresses directly the inertial angular acceleration of the Sun, is a useful discriminant for the closest approaches to the barycenter when its values are significantly different from zero.

In Fig. 2, we also present the solar activity history as characterized by the aforementioned proxy sunspot number reconstruction, SN, by Usoskin et al. (2014). The known historical GM of the last millennium and their respective durations are marked by vertical dashed lines. We emphasize that such timings for the GM events are independent of both, the SN reconstruction and the calculated PE values, and they were taken from classical/nominal values found in the literature (see e.g., Fairbridge and Shirley, 1987). We also plotted the observed number of sunspots, roughly in yearly or annual-mean resolution, from 1749 AD to date in Fig. 2. From Fig. 2, we can observe pulses of PE_{tot} minima (i.e., also refers to them simply as *pulses* throughout our paper) at or prior to the beginning of all five GM events. In addition, we can also see pulses around 1150 AD, related to the Medieval Optimum, and also the pulse starting around 1950 AD, related to the plausible, candidate ongoing solar prolonged minimum. In what follows, we assign a name to each pulse according to the nearest GM event e.g., MP for the Maunder pulse. Or as in the case of the pulses at around 1150 AD (between OM and WM) and at around 1990 AD, we call them MeP (for Medieval Pulse) and OnP (for Ongoing Pulse), respectively.

Basically we can observe two classes of pulses. The pulses that composed of a series of three big drops in PE and those composed of a large number of drops in PE values. Our interpretation of such dynamical phenomena is as follows. When the giant planets are quasi-aligned (at about 1632 AD, 1811 AD and 1990 AD, separated by ~ 179 yr), the Jupiter–Saturn–Uranus conjunctions are very effective in decreasing PE (i.e., in decreasing r_B distances) because Uranus and Neptune continue to be aligned, and this occurs within a slightly shorter time span than the S–U period (~ 39 – 40 yr) because of Jupiter’s co-alignment with Saturn. Then similar replicas in drops of PE storage are produced at these times (Cionco and Compagnucci, 2012).

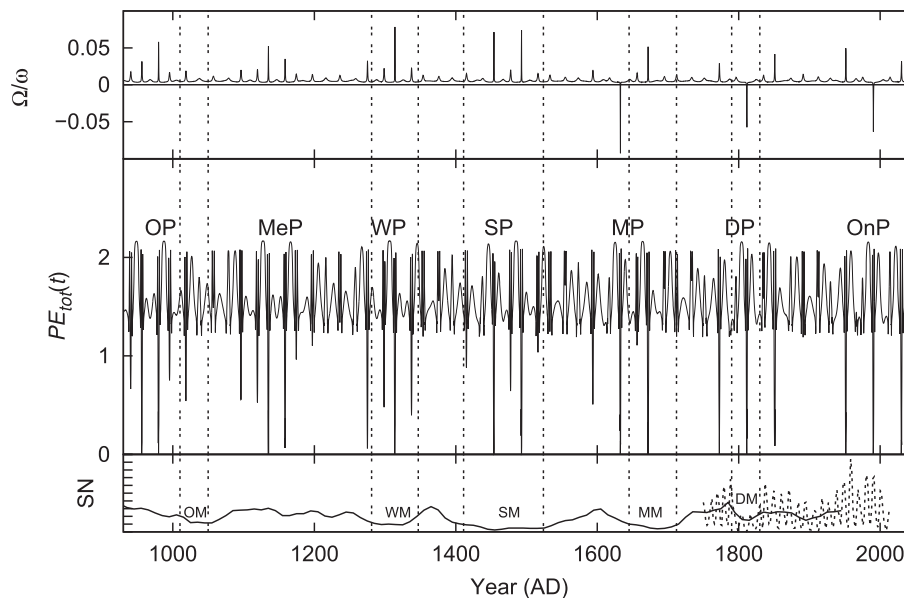


Fig. 2. Translational–rotational parameter Ω/ω ratio (top panel); potential energy, PE_{tot} (middle panel), stored in the Sun at the three key locations, and proxy sunspot number, SN, reconstructed by Usoskin et al. (2014) (solid line; bottom panel) covering the last millennium. The yearly observed SN (dashed-line) are also indicated from 1749–2013 in the bottom panel. The pulses of PE_{tot} minima are produced by the closest approaches of the Sun to the barycenter. In addition, at these epochs, Ω/ω ratio has its maximum values. The previously known GM events (i.e., OM, WM, SM, MM, and DM) from solar activity proxies are marked. The names of the pulses of PE_{tot} minima between Oort Minimum and Wolf Minimum (MeP) and the related ongoing prolonged minima (OnP) are also labeled as well as those corresponded directly to historical GM events.

When the planets are not so “exactly” aligned (e.g., at around 1300 AD and 1450 AD), the Sun is more free to be susceptible to the perturbations by the Jupiter–Saturn orbital dynamics. In fact, the Jupiter orbital period is clearly imprinted on PE_{tot} and it is visible around 1315 AD; then during such times, we can have more PE_{tot} dips than during times when the SBM is in retrograde phase. It is worth noting that, whereas SBM is repeated about every 179 yr (as confirmed by Fairbridge and Shirley (1987)), the planetary positions and the r_B values are never exactly the same (the planetary periods are not commensurables, i.e., they are not in mean-motion resonances), we do not have the same exact extrema in r_B values for each and every 179 yr; i.e., the occurrence of minimal values of r_B change over the time. Therefore, minima in PE do not recur exactly and periodically every 179 yr.

From Fig. 2, we note that whereas the pulses related to MP, DP, and OnP are repeated every 179 yr, the biggest drops in PE_{tot} at SP (which is also clearly observed as a major similar spike in Ω/ω panel in Fig. 2) occurs 139 yr before 1632 AD (i.e., at around 1493 AD), and also at ~ 39 yr before this date (i.e., at around 1454 AD), as both events are related to the co-alignment period of Saturn–Uranus–Jupiter (S–U–J). Then going back in time, again at about 140 yr before this last closest approach, the minima of WP occurs at around 1314 AD. At around 1135 AD, 179 yr before, the MeP minima occurs. Finally, 155 yr before, the big drop in PE_{tot} related to the OP event occurs at around 980 AD. The key lesson from Fig. 2 we wish to convey is the fact that even the seemingly clock-like dynamics of the orbital motions of the solar system bodies is really complex and may defies any simplistic description and prevent conclusion on any strictly periodic phenomena and physical processes involved.

As previously commented and highlighted in Cionco and Compagnucci (2012), the duration of the first class of the quasi-periodic pulses takes about 80 yr ($\sim 2 \times$ S–U–J period before and after the great alignment), and this result also holds for the second class of non-periodic pulses shown and discussed here; with the exception of SP. As discussed above, this Spörer minimum-related pulse is in turn composed of two similar pulses, and the total duration is about 119 yr ($\sim 3 \times$ S–U–J period). This is very interesting, because Spörer Minimum seems indeed to be the most extended GM event of the last millennium. All the PE pulses and minima are related to GM events, with the exception of MeP, which is related to the Medieval Optimum. Indeed, the ongoing Solar Cycle 24 maximum now appears to be the lowest in at least about 100 yr (see Hathaway, 2010; Petrovay, 2010; Tan, 2011; Livingston et al., 2012; Muñoz-Jaramillo et al., 2013). Upton and Hathaway (2014), for example, has recently compared Cycle 24 to the low activity during Cycle 14; therefore, OnP seems to be a plausible candidate related to a prolonged solar activity minimum event that is ongoing now. We add that such a timely perspective and insight is only possible from the detailed and careful study of SPI proposed here.

Taking into account the fact that big drops in PE are produced by the closest approaches of the Sun to the barycenter, we can expect that at the time of these pulses, the planets should impose a perceptible effect on the Sun internal dynamics because lesser PE is available than when the Sun’s orbital vantage point is far from the barycenter. We wish to note that our SPI picture here may be physically meaningful in that it also offer a natural explanation on why Grand Minima are more easily detected in solar activity proxies while the identification of the so-called Grand maxima of solar activity “is indeed challenging” as highlighted recently by Usoskin et al. (2014).

Therefore, a relationship between the Sun’s unique SBM at shorter barycentric distances and the occurrence of GM events, should be noted at the times of these low or minimum PE pulses. In order to evaluate this, we calculate the time interval (Γ) in which the Sun have $r_B < 0.65R_s$ (i.e., this is approximately the

distance at which the available $PE_{\nu}(0, 16R_s)$ drops significantly), around the pulse minima (which are clearly visible following the major spikes in Ω/ω ratio), during pulse duration:

$$\Gamma = \int_{r_{min}}^{0.65R_s} \frac{dr_B}{\dot{r}_B(t)}, \quad (9)$$

if t is in the corresponding PE pulse period.

From Table 1, we find that large Γ values, as they relate to all the GM events, are clearly observed or inferred (i.e., after all GM events are indeed described as “prolonged” solar activity minima) for the past millennium. This result suggests that, as the Sun spends appreciably more time at shorter barycentric distances, there are less PE available (specifically the $PE_{\nu}(0.16R_s)$ component) for interactions. We propose that GM events are directly related to this Γ time when the Sun spent an optimal duration with $r_B < 0.65R_s$. This optimal duration is discussed immediately below.

The shortest Γ time of about 25 yr is found during the MeP pulse at the Medieval Optimum and clearly, no solar activity minimum event has occurred. This result supports our idea for relating longer Γ (i.e., >25 yr) and GM events. The OnP pulse, that was initiated around 1951 AD also has a small Γ value, but its value of 30 yr is slightly larger than the MeP pulse. Taking into account the aforementioned evidence showing the current solar activity and solar cycle as rather atypical and/or unusual, we can suppose that a Γ value between 25 and 30 yr is the threshold value for a pulse to be a candidate GM event. Of course, the confirmation in the coming years about the nature of the current ongoing solar activity cycles of the past several decades will be a strong test for our proposed phenomenological rule.

In Fig. 3, we present our results for the next millennium. Particularly, another class of pulses are evident: almost all of these future PE pulses are related to the scenarios of retrograde solar motion but also with some very close approaches that loop around the barycenter (i.e., also visible as yielding both positive and negative spikes in the translational–rotational parameter Ω/ω ratio shown in the top panel of Fig. 3). These SBM configurations produce very symmetric peaks with similar minima in PE values, at around 2150 AD, 2310 AD and 2500 AD. The pulses around 2500 AD, 2700 AD and 2850 AD are more extended in durations, lasting for ~ 120 yr. All these three pulses pass our empirical criterion, using Γ time, to be considered as GM events as well as the first two GM with shorter durations. This is why we conclude that if our modeling of SPI together with our Γ rule are sound and essentially correct, then the ongoing millennium will have quite a number of periods and episodes of prolonged low solar activity phases. We do wish, however, to emphasize that this result in Fig. 3 does not constitute any proper scientific forecast or prediction of our future (see Armstrong, 2001) but instead it is merely the phenomenological extrapolation our modeling of the solar system orbital dynamics. In this sense, it is also useful to compare and contrast, though not entirely a one-to-one comparison, our SPI approach with the recent highlights of the prediction limits from solar dynamo modeling, as imposed by factors such as turbulent magnetic pumping (Guerrero and de Gouveia Dal Pinto, 2008; Karak and Nandy, 2012) and cross-equatorial flux transport (Cameron et al., 2013), to no more than about 5 yr ahead in time.

Table 1

The parameter, Γ , representing the times at which the Sun spends its orbital motion at barycentric distances $< 0.65R_s$ around each PE pulse. The names for these pulses follow the abbreviations discussed in the text and depicted in Fig. 2.

| Γ [yr] | 33.9 | 25.06 | 34.78 | 44.88 | 43.00 | 34.87 | 30.50 |
|------------------|------|-------|-------|-------|-------|-------|-------|
| PE_{tot} pulse | OP | MeP | WP | SP | MP | DP | OnP |

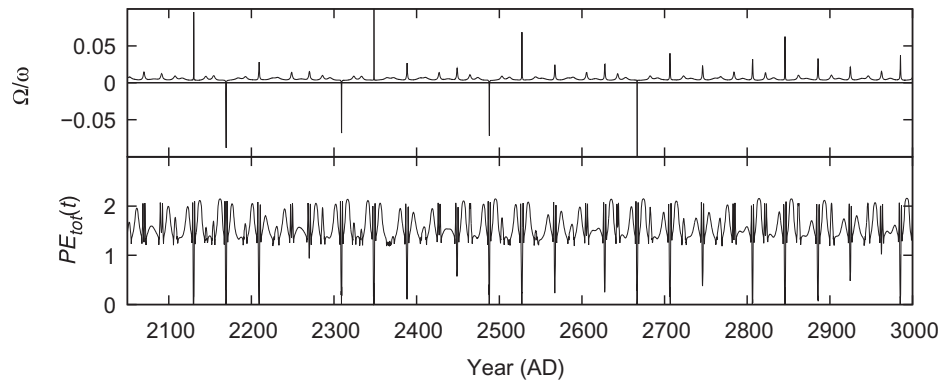


Fig. 3. Translational–rotational parameter Ω/ω and PE_{tot} stored in the Sun for 2050 AD to 3000 AD. We expect a larger number of candidate GM events because there are many more pronounced approaches of the Sun nearing the barycenter anticipated in the next one thousand years. The dynamical Γ parameter (see text for discussion of this important quantity) we calculated for these future candidate GM events give values similar to the GM events of the past millennium shown in Fig. 2.

5. Conclusions

Our new calculations confirm the previous early results of Cionco and Compagnucci (2012) by presenting a more complete calculation of the PE components specified in WP10; extending these first estimates to all GM events of the last millennium. The full orbital dynamic integration in our work clearly emphasizes an accurate accounting of the gravitational interactions of all the solar system bodies in order to capture the semi-regular but persistent perturbations on the internal operation of the rotating mass elements in the Sun. Our study of the pulses of PE_{tot} minima, the Γ parameter values, and in combination with the large excursions of the translational–rotational parameter Ω/ω ratio is able to offer a rather simple accounting for the timing and pre-warning of the known solar activity minima in the last 1000 yr. It is useful to remind that indeed these solar activity phases were called Grand Minima because of their extended durations of significantly weakened solar activity variations.

Our basic result is that the big pulses in PE are not only confined to epochs of great planetary alignments (i.e., at around 1632 AD; 1811 AD, 1990 AD), but also to all close approaches to the barycenter. We find that the time duration, represented by the dynamic parameter, Γ , in which the Sun spends at shorter barycentric distances within these pulses, seems to be a key parameter to select which PE pulses will produce a GM event. This proposal implies that the well-mixed radiative location is the key zone of this process, because PE minima are directly related to $PE_v(0.16R_s)$. On the other hand, this finding, in turn, suggests the GM events are not necessarily nor strictly periodic, it depends on the particular giant planets positions and configurations and the corresponding close approaches to the barycenter; although certain quasi-regular oscillations can be identified because the basic SPI physical mechanism is ultimately traced back to the solar system orbital dynamics

Finally, if our specified, tentative, rule for GM events with $\Gamma > 25$ to 30 yr is anywhere reasonable, we note that our Fig. 3 indeed shows that for the current millennium, there are several extended periods of prolonged and weakened solar activity phases that will likely have significant implications for Earth's climate (see e.g., Soon et al., 2014).

We conclude that a complimentary way, instead of being an alternative or independent method, for studying solar activity variation through the phenomenological approach of SPI advocated here is viable. Although the physical framework we used depends strictly on WP10's mechanism, we propose that such study may ultimately be able to add more significant insights to the real physical operation of the solar dynamo. We consider this work to be an

initial step worthy of further exploration rather than to be simply dismissed. The hunt for the complete set of SPI physical mechanisms must henceforth begin in earnest.

In defense of our SPI approach, we like to highlight the point that a full-fledge solar dynamo modeling effort, solving some versions of the magnetohydrodynamic equations, has thus far eluded any identification of specific timing for any of the known solar Grand Minima, including especially the Maunder Minimum (Soon and Yaskell, 2004). The SPI framework also seems to offer a natural explanation to the current debate concerning the continuous operations of the solar dynamo in exhibiting the decadal-and bi-decadal-like modulation of the solar activity indices, despite at a very low-amplitude modulation, during the Grand Minima intervals as recently discussed for the Maunder Minimum interval by Beer et al. (1998) and Miyahara et al. (2004).

The best analogy we like to put forth in arguing for the relevance and importance of this SPI effect is through the well-known and well-accepted Milankovitch Cycles of Ice Ages and Warm Interglacials that are rooted in the apparently “weak” or “insignificant” (again but *persistent* over ten to hundred thousand of years) perturbation of the Sun–Earth orbital geometry by giant planets like Jupiter and Saturn. Moreover, the SPI framework may eventually even permits accurate constraints on timing volcanic events dated in several tree-ring and ice-core chronologies as the solar-climatic-telluric relation has been suggested and not ruled out (see e.g., Odintsov et al., 2006). A good example is the date of 1454 AD for the PE_{tot} minimum we identified which may be coincidental with the recently identified Kuwae submarine volcanic eruption events around Vanuatu in the south Pacific (see Gao et al., 2006; Plummer et al., 2012).

Acknowledgements

RGC acknowledges the support of the UTN Grant PID-1351, “Forzantes Externos al Planeta y Variabilidad Climática”.

References

- Armstrong, J.S., 2001. *Principles of Forecasting*. Boston, Kluwer.
- Augustson, K., Brun, S., Miesch, M., Toomre, J., 2014. *The Astrophysical Journal*, submitted for publication. arXiv:1310.8471v1.
- Beer, J., Tobias, S., Weiss, N., 1998. *Solar Phys.* 181, 237.
- Brandenburg, A., 2013. *Non-linear and chaotic dynamo regimes*. In: Kosovichev, A.G., de Gouveia Dal Pino, E.M., Yan, Y. (Eds.), *Solar and Astrophysical Dynamics and Magnetic Activity*, Proceedings of the International Astronomical Union, IAU symposium, vol. 294, p. 387.
- Cameron, R.H., Dasi-Espuig, M., Jiang, J., Isik, E., Schmitt, D., Schussler, M., 2013. *Astron. Astrophys.* 557, A141.
- Chambers, J.E., 1999. *Mon. Not. R. Astron. Soc.* 304, 793.

- Charvátová, I., 2000. *Ann. Geophys.* 18, 399.
- Charvátová, I., 2009. *New Astron.* 14, 25.
- Choudhuri, A.R., Karak, B.B., 2012. *Phys. Rev. Lett.* 109, 171103.
- Cionco, R.G., 2012. *IAU Symp.* 286, 410.
- Cionco, R.G., Compagnucci, R.H., 2012. *Adv. Space Res.* 50, 1434.
- Fairbridge, R.W., Shirley, J.H., 1987. *Solar Phys.* 110, 191.
- Fienga, A., Manche, H., Laskar, J., Gastineau, M., Verma, A., 2013. INPOP new release: INPOP10e. ArXiv e-prints. arXiv:1301.1510.
- Gao, C., Robock, A., Self, S., Witter, J.B., Steffenson, J.P., Clausen, H.B., Siggaard-Andersen, M.-L., Johnsen, S., Mayewski, P.A., Ammann, C., 2006. *J. Geophys. Res. Atmos.* 111, 12107.
- Gizon, L., and 34 colleagues., 2013. *Proc. Natl. Acad. Sci. (USA)* 110, 13267.
- Gokhale, M.H., 1998. *Bull. Astron. Soc. India* 26, 173.
- Gough, D.O., 1990. *Philos. Trans. R. Soc. London A330*, 627.
- Gough, D.O., 2002. How is solar activity influencing the structure of the Sun? In: *From Solar Min to Max: Half a Solar Cycle with SOHO*, Proceedings of SOHO 11 Symposium, (European Space Agency SP-508), p. 577.
- Guerrero, G., de Gouveia Dal Pinto, E.M., 2008. *Astron. Astrophys.* 485, 267.
- Hathaway, D.H., 2010. *Living Rev. Sol. Phys.* 7, article 1 <<http://solarphysics.livingreviews.org/Articles/lrsp-2010-1/>> .
- Hazra, S., Passos, D., Nandy, D., 2014. A stochastically forced time delay solar dynamo: Self-consistent recovery from a Maunder-like Grand Minimum necessitates a mean-field alpha effect. *Astrophys. J.* submitted for publication. arXiv:1307.5751v3.
- Javaraiah, J., 2005. *Mon. Not. R. Astron. Soc.* 362, 1311.
- Jose, P.D., 1965. *Astron. J.* 70, 193.
- Jouve, L., Proctor, M.R.E., Lesur, G., 2010. *Astron. Astrophys.* 519, A68.
- Juckett, D.A., 2000. *Solar Phys.* 191, 201.
- Karak, B.B., Nandy, D., 2012. *Astrophys. J. Lett.* 761, L13.
- Landscheidt, T., 1999. *Solar Phys.* 189, 415.
- Licht, A., Hulot, G., Gallet, Y., Thébaud, E., 2013. *Phys. Earth Planet. Inter.* 224, 38.
- Livingston, W., Penn, M.J., Svalgaard, L., 2012. *Astrophys. J. Lett.* 758, L8.
- Maunder, E.W., 1894. *Knowledge* 17, 173.
- Miyahara, H., Masuda, K., Muraki, Y., Furuzawa, H., Menjo, H., Nakamura, T., 2004. *Solar Phys.* 224, 317.
- Muñoz-Jaramillo, A., Balmaceda, L.A., deLuca, E.E., 2013. *Phys. Rev. Lett.* 111, 0411106.
- Odintsov, S., Boyarchuk, K., Georgieva, K., Kirov, B., Atanasov, D., 2006. *Phys. Chem. Earth* 31, 88.
- Olemsky, S.V., Kichatinov, L.L., 2013. *Astrophys. J.* 777, 71.
- Paluš, M., Kurths, J., Schwarz, U., Seehafer, N., Novotná, D., Charvátová, I., 2007. *Phys. Lett. A* 365, 421.
- Passos, D., Nandy, D., Hazra, S., Lopes, I., 2014. *Astron. Astrophys.* 563, A18.
- Perryman, M.A.C., Schulze-Hartung, T., 2011. *Astron. Astrophys.* 525, A65.
- Petigura, E.A., Howard, A.W., Marcy, G.W., 2013. *Proc. Natl. Acad. Sci. (USA)* 110, 19273.
- Petrovay, K., 2010. *Living Rev. Sol. Phys.* 7, article 6 <<http://solarphysics.livingreviews.org/Articles/lrsp-2010-6/>>.
- Pipin, V.V., 1999. *Astron. Astrophys.* 346, 295.
- Pipin, V.V., Sokoloff, D.D., Usoskin, I.G., 2012. *Astron. Astrophys.* 542, A26.
- Pipin, V.V., Sokoloff, D.D., Usoskin, I.G., 2013. Waldmeier relations and the solar cycle dynamics by the mean-field dynamos. In: Kosovichev, A.G., de Gouveia Dal Pinto, E.M., Yan, Y. (Eds.), *Solar and Astrophysical Dynamos and Magnetic Activity (IAU Symposium No. 294)* <<http://arxiv.org/abs/1211.2423>> .
- Plummer, C.T., Curran, M.A.J., van Ommen, T.D., Rasmussen, S.O., Moy, A.D., Vance, T.R., Clausen, H.B., Vinther, B.M., Mayewski, P.A., 2012. *Clim. Past* 8, 1929.
- Scafetta, N., 2012. *J. Atmos. Sol. Terr. Phys.* 80, 296.
- Soon, W., Yaskell, S., 2004. *The Maunder Minimum and the Variable Sun–Earth Connection*. World Scientific Publishing, Singapore.
- Soon, W., Velasco Herrera, V.M., Selvaraj, K., Traversi, R., Usoskin, I., Chen, A.C.-T., Lou, J.-Y., Kao, S.-J., Carter, R.M., Pipin, V., Severi, M., Becagli, S., 2014. *Earth Sci. Rev.* 134, 1.
- Souami, D., Souchay, J., 2012. *Astron. Astrophys.* 543, A133.
- Spiegel, E.A., 2009. *Space Sci. Rev.* 144, 25.
- Spiegel, D.S., Raymond, S.N., Dressing, C.D., Scharf, C.A., Mitchell, J.L., 2010. *Astrophys. J.* 721, 1308.
- Stenflo, J.O., 2013. *Astron. Astrophys. Rev.* 21, 66.
- Tan, B., 2011. *Astrophys. Space Sci.* 332, 65.
- Tan, B., Cheng, Z., 2013. *Astrophys. Space Sci.* 343, 511.
- Tobias, S.M., Weiss, N.O., Kirk, V., 1995. *Mon. Not. R. Astron. Soc.* 273, 1150.
- Upton, L., Hathaway, D.H., 2014. *Astrophys. J.* 780, article 5.
- Usoskin, I.G., 2013. *Living Rev. Sol. Phys.* 10, article 1 (updated March 21, 2013) <<http://www.livingreviews.org/lrsp-2013-1>> .
- Usoskin, I.G., Solanki, S.K., Kovaltsov, G.A., 2007. *Astron. Astrophys.* 471, 301.
- Usoskin, I.G., Hulot, G., Gallet, Y., Roth, R., Licht, A., Joos, F., Kovaltsov, G.A., Thebaud, E., Khokhlov, A., 2014. *Astron. Astrophys.* 562, L10.
- Weiss, N.O., 2011. Solar and stellar dynamos. In: Brummell, N.H., Brun, A.S., Miesch, M.S., Ponty, Y. (Eds.), *Astrophysical Dynamics: From Stars to Galaxies*, Proceedings of the International Astronomical Union, IAU symposium, vol. 271, p. 247.
- Wolff, C.L., Patrone, P.N., 2010. *Solar Phys.* 266, 227.